Strategies for employing surface plasmons in near-field optical readout systems

Choon How Gan and Greg Gbur

Department of Physics and Optical Science
University of North Carolina at Charlotte
Charlotte, NC
gjgbur@uncc.edu

Abstract: The enhanced transmission of light through subwavelength-size holes in a metal plate is well-known to be associated with surface plasmons. We have undertaken a systematic theoretical study of several strategies for applying these plasmon effects in a near-field optical readout system using an exact Green's tensor formulation. Based on the results of our simulations with light of wavelength $\lambda = 500$ nm, data structures separated by 120 nm could be clearly resolved, and asymmetries of about ± 10 nm in the optical readout system could be tolerated without serious degradation of the performance. Advantages and disadvantages of each strategy are discussed.

© 2006 Optical Society of America

References and links

1. E.Betzig, J.K. Trautman, R.Wolfe, E.M. Gyorgy, P.L. Finn, M.H. Kryder and C.H. Chang, "Near-field magneto-optics and high density data storage," App. Phys. Lett. **61**, 142 (1992).
2. J. Tominaga, T.Kikukawa, M. Takahashi and R.T. Phillips, "Structure of the optical phase change memory alloy, Ag-V-In-Sb-Te, determined by optical spectroscopy and electron diffraction," J. Appl. Phys. **82**, 3214 (1997).
3. T.W. Ebbesen, H.J. Lezec, H.F. Ghaemi, T.Thio, P.A. Wolff, "Extraordinary optical transmission through sub-wavelength hole arrays," Nature **391**, 667 (1998).
4. T. Thio, K.M. Pellerin, R.A. Linke, H.J. Lezec, T.W. Ebbesen, "Enhanced light transmission through a single subwavelength aperture," Opt. Lett. **26**, 1972 (2001).
5. G. Gbur, H.F. Schouten and T.D. Visser, "Achieving superresolution in near-field optical data readout systems using surface plasmons," App. Phys. Lett. **87**, 191109 (2005).
6. L. Martín-Moreno, F.J. García-Vidal, H.J. Lezec, A. Degiron and T.W. Ebbesen, "Theory of highly directional emission from a single subwavelength aperture surrounded by surface corrugations," Phys. Rev. Lett. **90**, 167401 (2003).
7. K.C. Pohlmann, *The Compact Disc Handbook*, 2nd ed. (Oxford University Press, Oxford, 1992).
8. T.D. Visser, H. Blok and D. Lenstra, "Theory of polarization-dependent amplification in a slab waveguide with anisotropic gain and losses," IEEE J. Quantum Electron. **35**, 240 (1999).
9. H.F. Schouten, T.D. Visser, D. Lenstra and H. Blok, "Light transmission through a subwavelength slit: Wave-guiding and optical vortices," Phys. Rev. E **67**, 036608 (2003).
10. H.F. Schouten, T.D. Visser, G. Gbur, D. Lenstra and H. Blok, "Creation and annihilation of phase singularities near a subwavelength slit," Opt. Express **11**, 371 (2003).
11. H.F. Schouten, N. Kuzmin, G. Dubois, T.D. Visser, G. Gbur, P.F.A. Alkemade, H. Blok, G.W. 't Hooft, D. Lenstra and E.R. Eliel, "Plasmon-assisted two-slit transmission: Young's experiment revisited," Phys. Rev. Lett. **94**, 053901 (2005).
12. U. Schröter, S. Seider, S.Tode and D. Heitmann, "Surface plasmon reflection at edges and resonance effects in metal bars," Ultramicroscopy **68**, 223 (1997).

13. Y. Xie, A.R. Zakharian, J.V. Moloney and M. Mansuripur, "Transmission of light through slit apertures in metallic films," Opt. Express **12**, 6106 (2004).
14. M. Born and E. Wolf, *Principles of Optics*, 7th ed. (Cambridge University Press, Cambridge, 1999).
15. H.F. Schouten, T.D. Visser, G. Gbur, D. Lenstra and H. Blok, "The diffraction of light by narrow slits in plates of different materials," J. Opt. A: Pure Appl. Opt. **6**, S277 (2004).
16. F.J. García de Abajo and J.J. Sáenz, "Electromagnetic surface modes in structured perfect-conductor surfaces," Phys. Rev. Lett. **95**, 233901 (2005).

1. Introduction

There has been much interest in recent years in employing near-field optical techniques to overcome the diffraction limit in optical data recording and readout systems. Some possibilities which have been explored include near-field magneto-optics [1] and optical phase change techniques [2]. More recently, enhanced transmission through subwavelength-size hole arrays [3] and single subwavelength apertures [4] in metal plates has been observed, an enhancement generally credited to surface plasmons. Although it has been suggested that the phenomenon of enhanced transmission could be useful in improving near-field optical readout systems ('super compact disc systems'), very little work has been done to study such a possibility theoretically. In a recent paper [5], it was suggested that the interference and resonance effects of surface plasmons could both help and hinder the readout process, and that a careful design of such a readout system would be necessary to provide improvement.

In the present paper, we undertake a systematic theoretical study of surface plasmon effects in a near-field optical readout system using a Green's tensor formulation in a two-dimensional geometry, with a single slit in a metal plate used as a near-field probe. The detection process was simulated by calculating the total power reflected from the readout system. We consider one or more data structures ('pits' or 'bumps') on the surface of the data layer, taken to be silver. Furthermore, to study the effects of enhanced transmission and plasmon resonances we consider the effect of placing surface features on the metal plate, referred to as 'plasmon pits'. These pits allow the coupling of light to the surface plasmons, and have been used successfully in previous studies of enhanced transmission [4, 6].

We find that a number of different system configurations could be used to effectively employ surface plasmon effects in data readout. Each of these systems differs in the nature of the readout process, and each has its own unique advantages and disadvantages. In the optimal configurations, data structures with a minimum separation of 120 nm (with wavelength $\lambda = 500$ nm) can be clearly resolved. Because construction of nanoscale devices will inevitably involve some imperfections, we have also undertaken a limited study of the susceptibility of the readout systems to asymmetries in the position of the plasmon pits. It is found that asymmetric positioning of about ± 10 nm can be tolerated without any serious degradation in performance.

We describe the proposed configurations for near-field optical readout in section 2, followed by a description of the Green's tensor formulation used in our simulations in section 3. Section 4 discusses the optimization of the different configurations and the effectiveness of the data readout. Finally in section 5, we discuss the advantages and disadvantages of each strategy.

2. Proposed Strategies for Near-field Optical Readout

We consider several configurations of a reflection readout system, in which a monochromatic field is normally incident on a slit in a metal plate, and readout is achieved by measuring the total power reflected from the system. The basic structure of each configuration is illustrated in Fig 1. Monochromatic light of wavelength $\lambda = 500$ nm is normally incident upon a silver plate of finite conductivity and thickness $t_2 = 100$ nm, which contains a single subwavelength slit of width a. The metal plate is situated a short distance $t_3 = 30$ nm away from a semi-infinite data

layer and serves the role of the optical disc. The position of the plasmon pits from the center of the slit is specified by γ. We shall only consider plasmon pits on the dark side of the plate in the proposed configurations, as it has been determined in Ref. [5] that plasmon pits on the illuminated side have detrimental effects on the performance of a reflection readout system, despite the fact that they enhance the amount of light coupling into the slit.
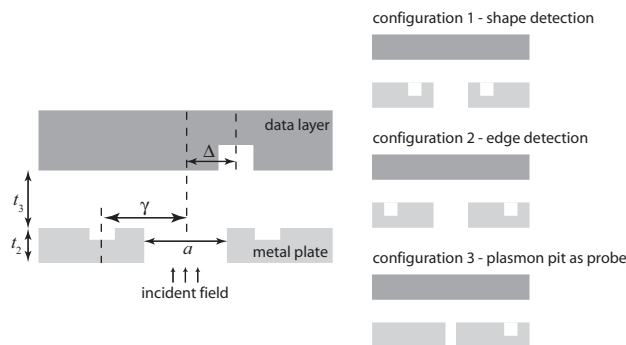

Fig. 1. Illustration of the three readout system configurations studied, and the relevant parameters used to quantify them. Configurations 1 and 2 only differ in the position of the plasmon pits, while configuration 3 has a different slit width and only a single plasmon pit.

Our preliminary studies suggested that three distinct strategies might be used to perform optical readout, and each of these strategies led to its own system configuration:

1. A configuration designed to accurately map the shape of the data structures on the disc. Here the system response must be roughly proportional to the distance of the data surface from the metal plate. This is the strategy adopted in an earlier study [5].

2. A configuration designed to detect only the edges of the data structure. This configuration assumes that the binary data is encoded only at the edges of a data pit, similar to the method in which conventional compact discs are encoded [7].

3. A configuration in a plasmon pit is itself used as the near-field probe, and the slit acts only as a source/receiver of plasmons.

Configuration 1 and configuration 2 differ only in the position of the plasmon pits from the center of the slit, γ. For configuration 1, the objective is to keep the electromagnetic energy localized in the immediate vicinity of the slit, and so γ is kept relatively small to suppress oscillations in the reflected power due to plasmon travelling modes and waveguide modes between the plate and data layer. For configuration 2, this condition on γ is relaxed to allow plasmon standing waves to build between the slit and the plasmon pits; because the fields of surface plasmons are strongest near the edges of the data structure[12, 13], enhancing the plasmon resonances should enhance the response of the system to the edges of the data structure. For both configurations, the plasmon pit width is 50 nm, and the slit width $a = 25$ nm. The data pit is taken to be 50 nm wide and 25 nm deep. The optimal choice of γ for both configurations is to be determined by simulation.

In configuration 3, only one plasmon pit is present, and the slit width is taken to be 10 nm. The size of the data pit is taken to be 50 nm wide and 50 nm deep, different from that in configurations 1 and 2. To enhance the resonating effects, the size of the data pit is made identical to that of the plasmon pit. We expect that, when the plasmon pit and data pit coincide, they act together to form a cavity, causing the field within to resonate strongly. The slit acts merely as

a plasmon source and collector for this case. The slit width, however, is kept as thin as seems practical; for large values of a, the system would behave similarly to configurations 1 and 2.

In looking for the optimal readout system, we consider mainly two criteria: the readout contrast (the percentage difference in reflected power when a pit is near the slit versus when none is present) and the resolution (the minimum separation of adjacent data pits that the readout system can resolve). The readout contrast is defined as the percentage difference in reflected power P when the data structure is present and absent, i.e.

$$\text{contrast} \equiv \left| \frac{P_{\text{data}} - P_{\text{no data}}}{P_{\text{no data}}} \right|. \tag{1}$$

It is to be noted that readout contrast indicates nothing about the overall strength of the reflected signal, which will be weak due to the subwavelength size of the slit. For resolution, we use a criterion stricter than the Rayleigh criterion [14, Sec. 7.6.3], and define two data structures as just resolved when the reflected power returns to the background level between the structures. We use a stricter criterion due to the previously-mentioned weakness of the reflected signal.

It is expected that imperfections in the nanofabrication of any realistic readout sytem could result in asymmetries of the plasmon pits. We have, therefore, also studied the tolerance to structure asymmetries in the first two configurations. Of particular interest is how the readout characteristics change when the position of the plasmon pits is made asymmetric.

3. The Green's Tensor Formulation

The Green's tensor formulation allows for an exact numerical solution of Maxwell's equations. The method involves the numerical solution of a domain integral equation [8, 9] for the electric field of the form,

$$E_i(x,z) = E_i^{(inc)}(x,z) - j\omega \int_D \Delta\varepsilon(x',z') G_{ij}^E(x,z;x',z') E_j(x',z') dx' dz' \tag{2}$$

where E_i represents the ith component ($i = x,y,z$) of the total electric field, $E_i^{(inc)}$ represents the incident field which would propagate in the system in the absence of the slit, data structures and plasmon pits, G_{ij}^E is the Green's tensor of the ideal layered medium, which can be calculated exactly (to within a spatial Fourier transform), and ω is the angular frequency of the field. The integral is over all regions D (slit, data structure, plasmon pits) in which the the system deviates from the ideal layered geometry. $\Delta\varepsilon$ is the difference in permittivity between the 'deviant' regions and the background system.

This equation can be solved numerically within the deviant regions by the collocation method with piecewise-constant basis functions. The field everywhere else may then be calculated by substitution back into Eq. (2). Due to the invariance of the system along the y-direction, only TM-polarized (**H** perpendicular to the $x - z$ plane) incident fields will excite surface plasmons, and we restrict ourselves to this case.

The Green's tensor method was employed to numerically analyze the effect of surface plasmons on the ability to detect and resolve individual data pits on the surface of an optical disc. The detection process was simulated by calculating the total power scattered from the readout system, subtracting the power which would be directly reflected back from a smooth planar surface. Such a system could be implemented in practice by measuring only power scattered in directions away from the normal to the surface.

4. Optimization of the readout systems

In attempting to design a readout system which uses surface plasmon effects optimally, one must consider the variation of a daunting number of parameters: the metal plate material, the

data layer material, the slit width, the plasmon pit size and location, the data structure size. We focus on optimizing a limited number of system properties that most directly relate to the effectiveness of the selected readout geometries.
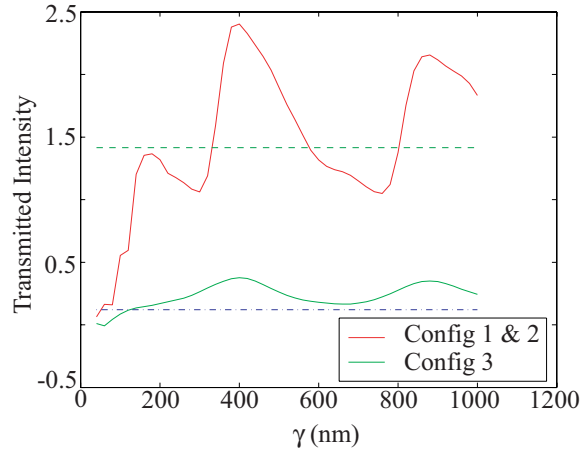

Fig. 2. Normalized transmission through the metal plate for the different readout configurations. The red curve indicates the transmission for configurations 1 and 2, while the green curve indicates the transmission for configuration 3. The dashed lines indicate the transmission in the absence of the plasmon pits. The transmission is roughly a periodic function of γ.

The position of the plasmon pits affects both the amount of energy transmitted through the system and the qualitative behavior of the readout. The transmission was calculated for the metal plate in the absence of the data layer for various values of γ. The definition of the transmission coefficient of the slit consists of two parts [10]: the first is the integral of the normal component of the time-averaged Poynting vector S over the slit, and the second is the difference of the normal components of the time-averaged Poynting vector and that of the Poynting vector in the absence of the slit, S^{inc}, integrated over the dark side of the plate (i.e. not the region of the slit). The result is normalized by the normal component of $S^{(0)}$, the Poynting vector of the field emitted by the source and impinging on the slit. This may be written as

$$T \equiv \frac{\int_{\text{slit}} S_z dx + \int_{\text{plate}} (S_z - S_z^{\text{inc}}) dx}{\int_{\text{slit}} S_z^{(0)} dx}. \tag{3}$$

The subtraction in the second integral of the numerator corrects for the small part of the incident field which may evanescently tunnel through the plate itself. A transmission greater than unity roughly indicates more light is passing through the slit than is geometrically incident upon it.

The results of the transmission calculation are shown in Fig. 2. The red line indicates the parameters that define system 1 and 2, while the green line indicates the parameters that define system 3. It can be seen that the transmission is roughly periodic as a function of the plasmon pit position; this is due to the standing wave nature of the plasmons between the pit and the slit (see, for instance, Ref. [11]). To prevent a similar standing wave from appearing between the slit and the data structure, the plasmon pits should be kept as close to the slit as possible. The transmission for configurations 1 and 2 has a local maximum in the range between $\gamma = 100$ nm and $\gamma = 250$ nm, which suggests that the plasmon pits should be taken to lie within this range. For configuration 3, the transmission did not increase substantially as a function of γ.

The qualitative behavior of the readout system was then studied by examing the response of the system to data structures for various values of γ. The simulations show gradual transitions

from the well-behaved readout reflectivity for configuration 1, to the growth of the oscillations for configuration 2, when γ is increased gradually from 60 nm to 140 nm, as is observed in Figs. 3, 4, and 6.
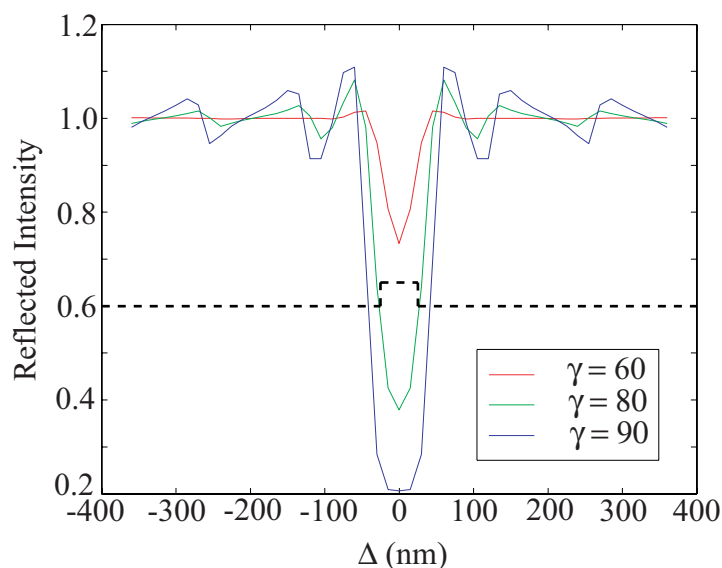

Fig. 3. Readout contrast for a single data pit, for various values of γ. The slit width is $a = 25$ nm, as used for configurations 1 and 2. The dashed line indicates the shape of the data pit.

For small γ (60 − 100 nm), as shown in Figs. 3 and 4, the reflected power exhibits dips when the data structures are detected by the readout slit, as expected since the presence of the pits reduces the amount of backscattering to the readout slit as compared to the case when the pits are not present. An optimal contrast ratio of about 60% is acheived when the data pit is detected for $\gamma = 80$ nm, as shown in Fig. 3. Figure 5 shows the electric field intensity distribution for various positions of the data pit in configuration 1 for $\gamma = 80$ nm. It can be seen from the movie that the field is mostly confined to the region between the plasmon pits.

For larger γ (110 − 140 nm), as shown in Figs. 4 and 6, the reflected power exhibits strong resonances when the edges of the pits are detected by the readout slit. From Fig. 4, an optimal contrast ratio of about 700% is achieved when the edges are detected for $\gamma = 120$ nm. As the plasmon effects are most intense at the edges where the field tends to accumulate, the field resonates strongly when the edges of the pits coincide with the readout slit. Figure 7 shows the electric field intensity distribution for various positions of the data pit in configuration 2; it can be seen that the field intensity is strongest when the edges of the data pit are in the neighborhood of the slit.

Beyond $\gamma = 160$ nm, either the resonances are too weak to provide useful data detection or additional spurious resonances appear due to plasmon reflection from the data structure.

For configuration 3, we observe again that the oscillations in the regions around the slit, plasmon pit, and data pits grow gradually as γ is increased from 60 − 180 nm, as seen in Figs. 8 and 9. The simulations suggest that the optimal γ in this case is 120 nm, with a contrast ratio of about 280%. Figure 10 shows the electric field intensity distribution for various positions of the data pits in configuration 3 for $\gamma = 120$ nm. An extremely strong resonance is created when the data pit and the plasmon pit positions coincide.

We also looked at the resolution of the three systems by examining their ability to resolve a pair of spatially separated data pits. Such a configuration represents a '1-0-1' arrangement
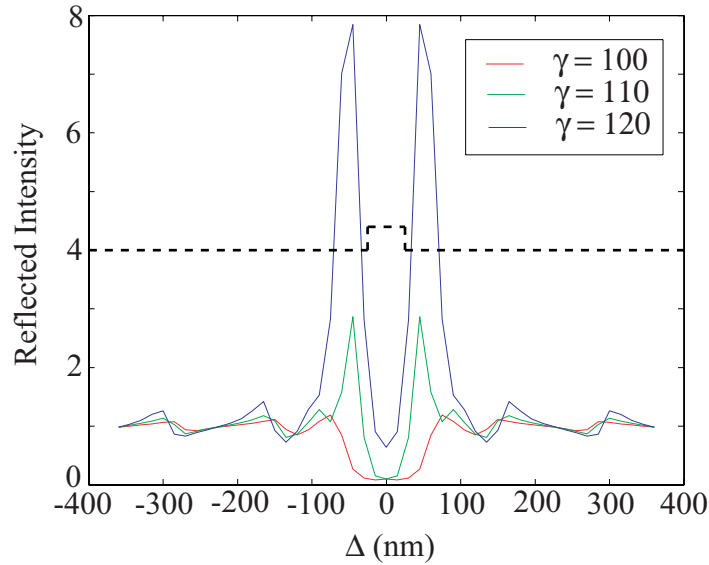
Fig. 4. Readout contrast for a single data pit, for larger values of γ. The slit width is $a = 25$ nm, as used for configurations 1 and 2. The dashed line indicates the shape of the data pit. The system now responds more to the edges of the data structure, rather than mapping the exact shape of the structure.
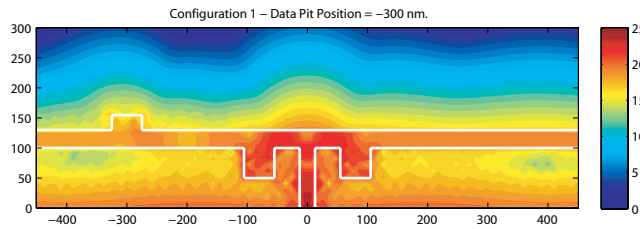

Fig. 5. (496 KB) Movie showing the intensity of the electric field in the vicinity of the readout system for various positions of the data structure, for configuration 1.

of three bits of information. For configuration 1, γ is taken to be 80 nm. For configurations 2 and 3, γ is taken to be 120 nm. The results in Figs. 11, 12, and 13 show two data structures just resolved according to our resolution criterion for the three configurations. It can be seen that two data pits separated by 120 nm, 220 nm, and 120 nm, could be resolved by each configuration, respectively.

5. Conclusion

We conclude by comparing the results for the three configurations, and discuss some advantages and disadvantages of each.

The highest contrast ratio of any system is found in configuration 2, with its excellent ratio of 700%. Its resolution is the worst of the three systems, however, at 220 nm. This system exhibits significant oscillations of the reflected power when the data structure is away from the vicinity of the slit, as can be seen in Fig. 4. Because of the high contrast ratio, these oscillations are not necessarily a problem.

Configuration 3 offers a better resolution, at 120 nm, and also has an excellent contrast ratio of 280%. However, this system uses a small slit size of 10 nm, and therefore has the lowest
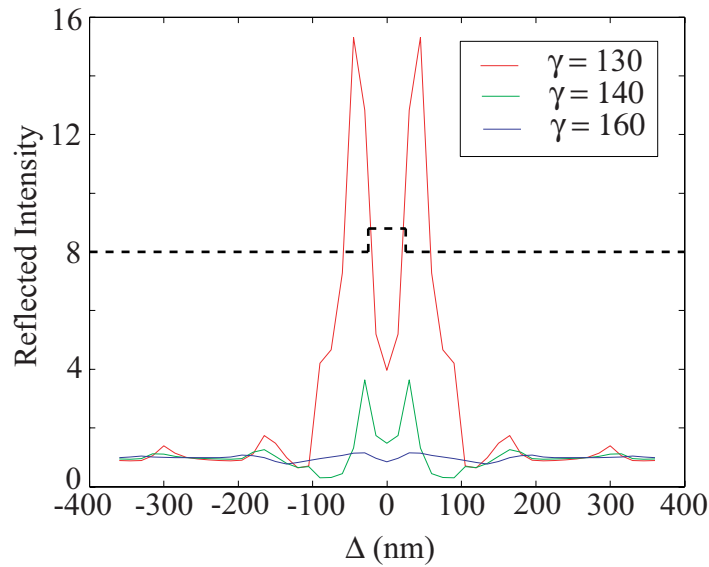
Fig. 6. Readout contrast for a single data pit, for even larger values of γ. The slit width is $a = 25$ nm, as used for configurations 1 and 2. The dashed line indicates the shape of the data pit. It can be seen that the readout contrast is again diminishing in this range.
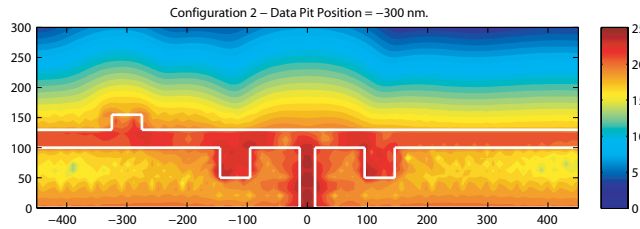

Fig. 7. (543 KB) Movie showing the intensity of the electric field in the vicinity of the readout system for various positions of the data structure, for configuration 2.

overall reflected power of any of the systems, which will make it more susceptible to system noise. Furthermore, as can be seen in Fig. 9, for certain values of γ significant oscillations in the reflected power can occur when the data structure is to the left of the slit. These oscillations could result in incorrect data readout.

Configuration 1 has a resolution comparable to configuration 3 (at 120 nm) but has the lowest contrast ratio (at 60%). It also exhibits very little oscillation in the reflected power.

Configuration 3 has an additional advantange in that it offers the simplest structure to fabricate. Only a single plasmon pit is required, and its position can vary widely and still offer good data readout, as seen in Figs. 8 and 9. Values of γ between 80 nm and 180 nm result in a significant contrast far above the oscillations of reflected power.

All these systems require rather precise specification of the slit width and the size and position of the plasmon pits. As any realistic fabrication will involve some imperfections, it is of interest to examine how sensitive the readout is to variations in parameters.

Both the readout contrast plots of configurations 1 and 3 are almost free of kinks or oscillations, though this is no longer true in the case of configuration 3 as the readout slit width increases, which can be seen from Fig. 14. Evidently for this configuration the variation in slit
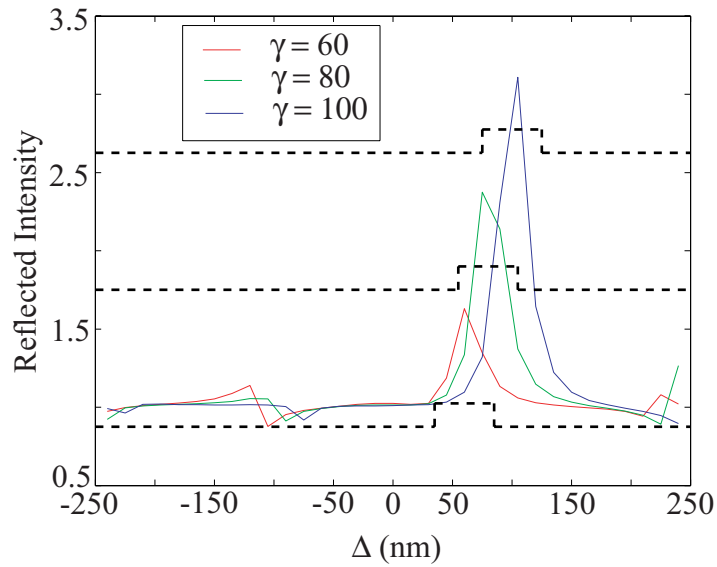
Fig. 8. Readout contrast for a single data pit, for configuration 3, with $a = 10$ nm. A resonance in the response of the system can be seen when the data structure passes the location of the readout plasmon pit.
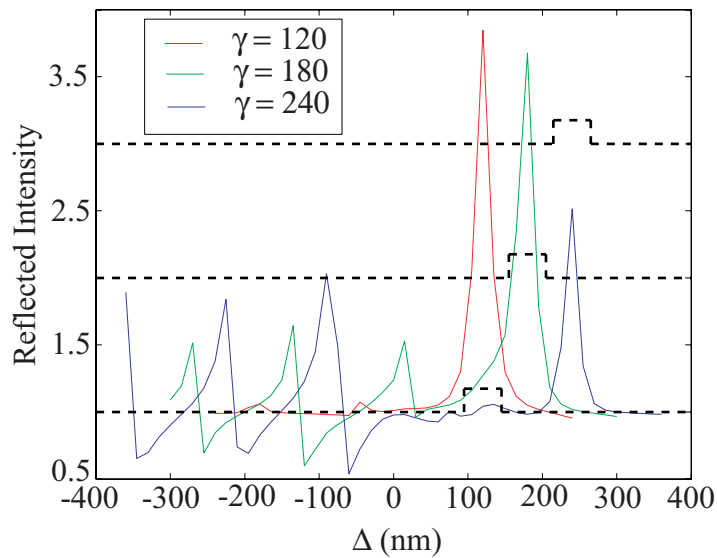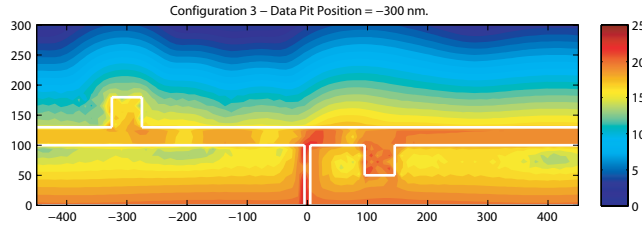

Fig. 9. Readout contrast for a single data pit, for configuration 3, with $a = 10$ nm. The contrast of the system improves in comparison with the previous figure, but significant oscillations appear when the data pit is on the side of the slit without the plasmon pit.

Fig. 10. (349 KB) Movie showing the intensity of the electric field in the vicinity of the readout system for various positions of the data structure, for configuration 3.
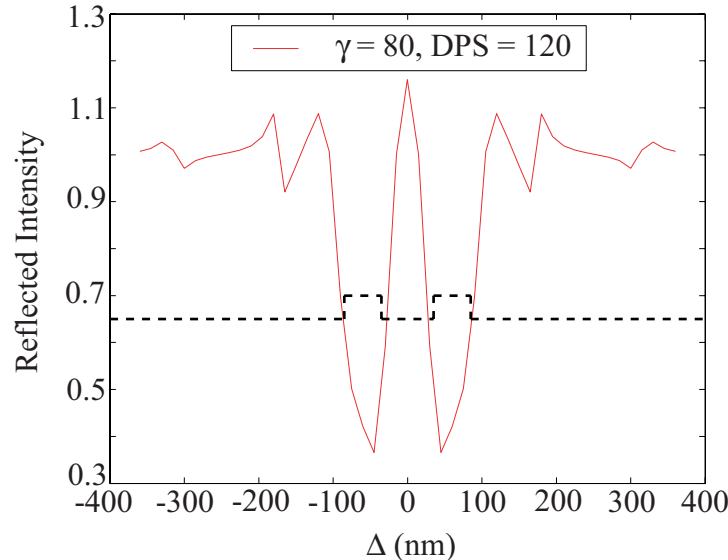
Fig. 11. Readout contrast for 2 data pits for configuration 1. With the pits separated by 120 nm, their shapes can be clearly distinguished in the reflected power.

width should be less than 5 nm. This is consistent with earlier observations that the transmission of light through subwavelength slits is strongly dependent on the slit width [15].

Configurations 1 and 2 require symmetry in the position of the plasmon pits. From the readout plots in Figs. 15 and 16, we see that for both configurations, a tolerance of about ±10 nm (70 − 90 nm for configuration 1, 110 − 130 nm for configuration 2) is acceptable, although the contrast ratio changes significantly.

It is to be noted that the results of this paper could be extended to a three-dimensional geometry in which the subwavelength-width slit is replaced by a subwavelength-radius hole. Such a configuration is the natural choice for a full experimental realization of a readout system, but is extremely difficult to simulate numerically. Our results give a qualitative idea of what behaviors could be expected in such a system. Also, there is no reason why a readout system could not be designed with a slit rather than a hole; superresolved readout would be limited to one dimension on the optical disc, but light throughput (and therefore signal-to-noise ratio) would be superior for the slit geometry, due to the absence of a cutoff wavelength in the slit for TM-polarized light.

It is also to be noted that one can use simple analytical models to qualitatively understand the behaviors of the readout systems. Such models have been used both to explain plasmonic
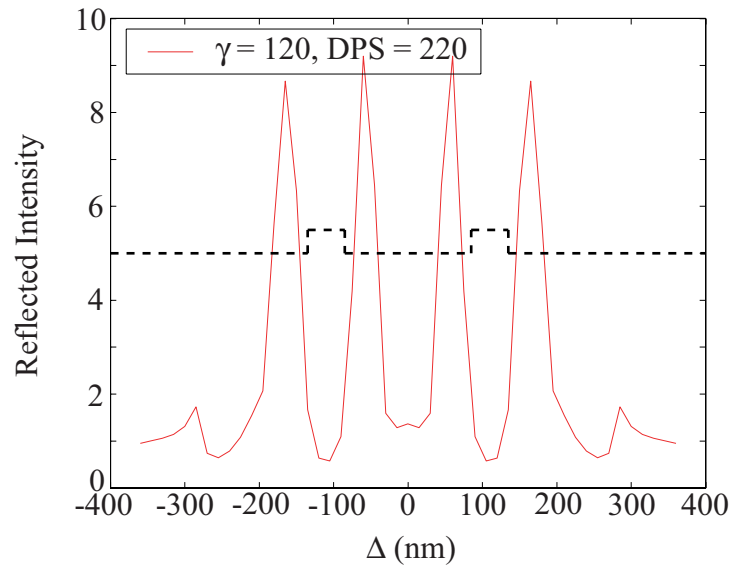
Fig. 12. Readout contrast for 2 data pits for configuration 2. The four edges of the data structures can be clearly resolved in the reflected power, with the pits separated by 220 nm.
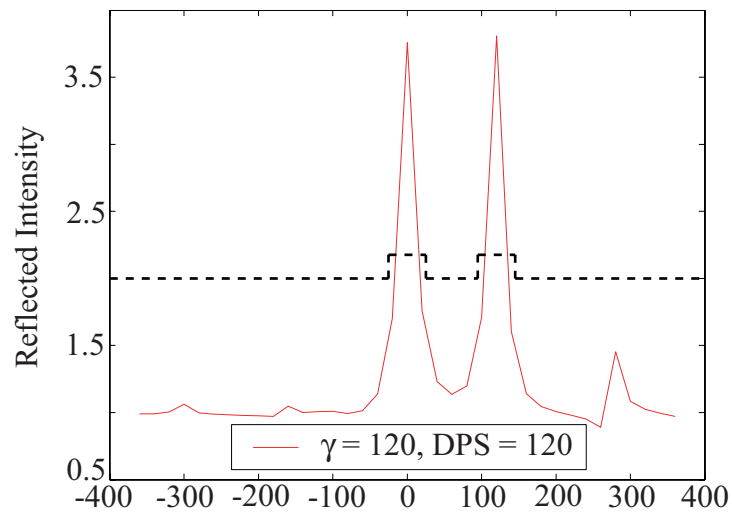

Fig. 13. Readout contrast for 2 data pits for configuration 3. The two pits can be resolved and are separated by 120 nm, though the contrast is not as good as for configuration 2.
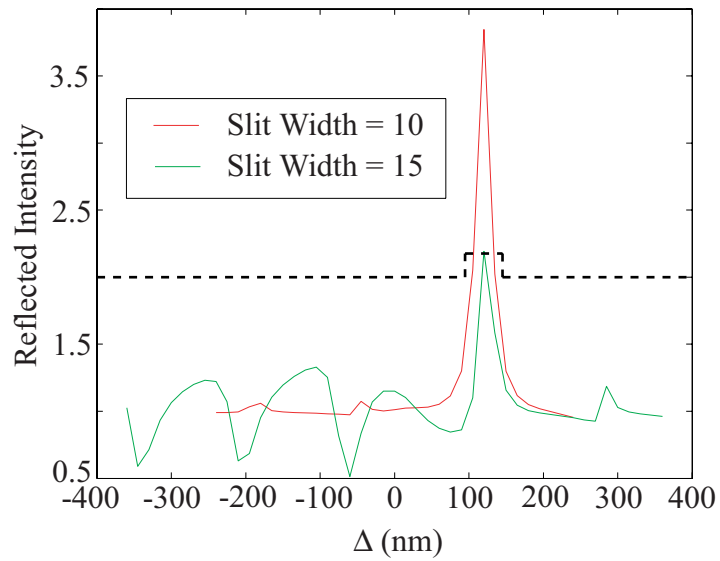
Fig. 14. Dependence of configuration 3 on the width of the slit. For even a 5 nm variation of slit width, the readout contrast is significantly reduced and the system oscillations dramatically increased.
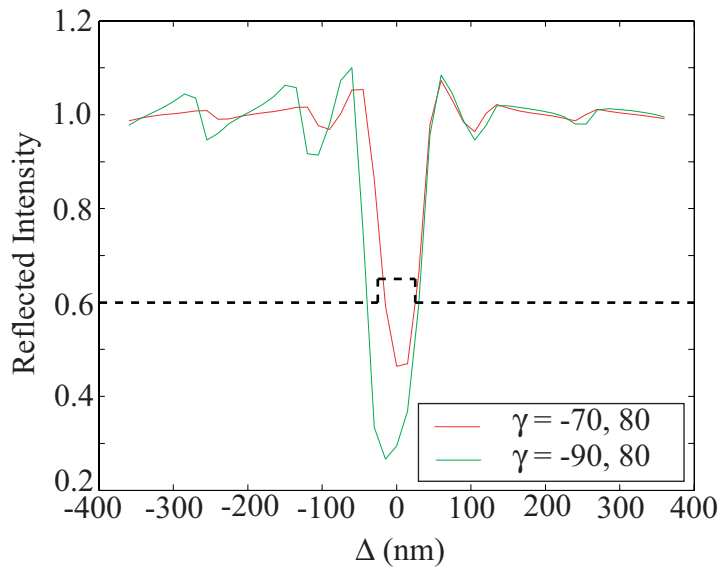

Fig. 15. Dependence of configuration 1 on the symmetry of the plasmon pits. It can be seen that a 10 nm variation in the position of one of the pits does not significantly affect the system performance.
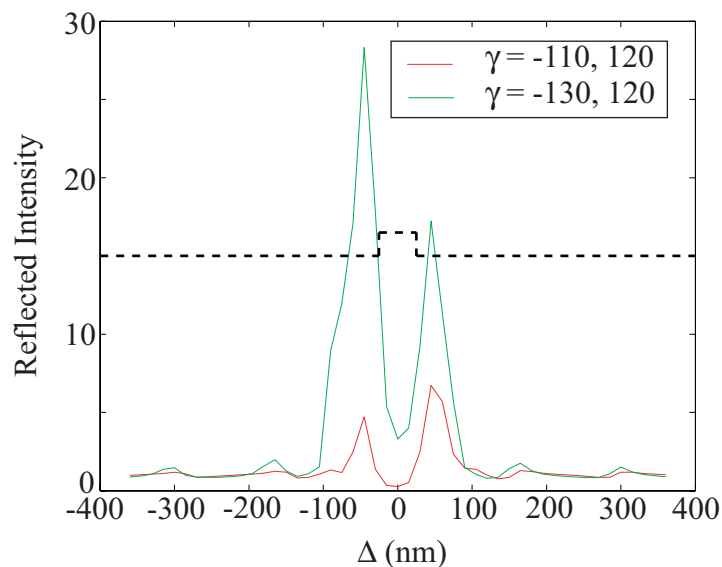
Fig. 16. Dependence of configuration 2 on the symmetry of the plasmon pits. The readout contrast is greatly affected by an asymmetry in the pit position of 10 nm, though readout is still possible.

enhanced transmission [11] as well as surface modes in metamaterials [16] and oscillations in plasmonic readout systems [5]. A quantitative analysis of the effectiveness of readout systems, however, will always require full electromagnetic simulation, due to the multiple interactions between the slit and the data structures.

Each of the systems described here has its own advantages and limitations. The choice of an optimal system will depend on what characteristics the designer finds most important (readout contrast, resolution, stability). In this study, we have shown that there is a significant flexibility in the application of enhanced transmission effects in near-field optical readout systems. It is hoped that these results will generally lead to a better use of plasmonic effects in near-field optical applications.

Acknowledgments